International Journal of Precision Engineering and Manufacturing (Accepted Manuscript)
(Published version DOI — https://doi.org/10.1007/s12541-021-00488-z)

Self-tuning Control for Articulated Robots Using the Plestan's Method

Maolin Jin[1] · **Jinoh Lee**[2] · **Kap-Ho Seo**[3] · **Jin-Ho Suh**[4]

Received: date / Accepted: date

Abstract A self-tuning controller is proposed for an articulated robot using the Plestan's method. To this end, we reconstruct the articulated robot dynamics exploiting the time-delay estimation (TDE) technique. The closed-loop error dynamics is described with sliding variables and TDE error; then, the Plestan's sliding mode based gain-adaptation law is incorporated with the TDE technique. The stability of the overall dynamics is proven in the sense of Lyapunov. As a result, self-tuning of the gain is realized through the sliding variable. When the TDE error increases due to the nonlinear effect such as friction, the adaptive gain is automatically adjusted to counteract the TDE error. Chattering can be avoided because the sliding mode based gain dynamics does not allow the gain increase to an excessively high value. The superiority of the proposed self-tuning controller is demonstrated by comparative experiments on a multiple joints robot setup.

Maolin Jin and Jinoh Lee contributed equally to this work. It was supported by the Ministry of Trade, Industry, and Energy (MOTIE, Korea) under Industrial Technology Innovation Program (Development of armored robot systems for personal protections of rescuemen and emergency management operations in the composite disaster site) under Grant 10067184.

✉ Jinoh Lee · jinoh.lee@dlr.de

[1]Human-centered Robotics Center, Korea Institute of Robotics and Technology Convergence (KIRO), Jigok-Ro 39, Pohang, Korea.
[2]Institute of Robotics and Mechatronics, German Aerospace Center (DLR), Münchener Str. 20, 82234 Weßling, Germany.
[3]Human Robot Interaction Center, Korea Institute of Robotics and Technology Convergence (KIRO), Jigok-Ro 39, Pohang, Korea.
[4]Department of Mechanical System Engineering, Pukyong National University, 45 Yongso-ro, Busan, Korea.

Keywords Adaptation · articulated robot · gain tuning · self-tuning · time-delay estimation (TDE)

1 Introduction

Attaining stable yet highly precise control of robots is of difficulty due to model uncertainties, nonlinearities, coupling dynamics effects, and unknown disturbances. Generally, exact robot dynamic model and its parameter identification are the prerequisites to obtain highly accurate tracking performance even in modern control theories. For example, calculations of the nonlinear terms of the robot dynamics equations are required for computed torque control [20], H_∞ switched adaptive control [23], and sliding mode control [6]. However, as robots are often designed with multiple degrees-of-freedom joints to dexterously execute required tasks, its dynamic identification process becomes entangled and laborious. In addition, identification of joint friction forces is challenging, because the friction forces are time-varying with hysteretic behaviors; indeed, implementation of these model-based controllers are highly complicated due to the calculation of the robot dynamics equations.

It is worth to notice that time-delay control (TDC) [8, 9, 29, 30] offers a robust, yet simple and efficient scheme without using the robot dynamics model. The TDC has shown extraordinary performance for robots with dynamic uncertainties and substantial parameter variations [11, 14, 16], overcoming the aforementioned constraints of dynamic model-based controllers. The TDC is a control technique that uses time-delay estimation (TDE) to cancel the system uncertainties and injects the desired error dynamics into the target plant.

Owing to the simplicity of the structure and robustness against uncertainties, the TDC also facilitates the implementation and maintenance of diverse control systems. Numerical efficiency of the TDE makes the TDC suitable for various real-time control applications and devices: robot manipulators [1, 2, 11, 12, 14, 16], a medical device [18], a shape memory alloy actuator [13], fuel cell systems [15, 28], aerial vehicles [19], cable-driven manipulators [24–27] and chaotic systems [10].

Many TDE-based control methods [1, 2, 10–16, 18, 19, 24–28] employ a constant gain matrix, whose elements are to be tuned by a trial-and-error method. Lately, it has been reported that the usage of *constant* gain values all the time is not good for the control performance and even causes instability, when the system parameters are substantially changing [4, 5]. To elaborate, the aforementioned control designs based on TDC use a constant diagonal gain matrix, $\overline{\mathbf{M}}$, which is physically associated with the inertia matrix of an articulated robot system with the multiple joints, $\mathbf{M}$. Note that although this gain matrix considerably affects overall control performance and stability, it is manually and heuristically tuned for each joints. Hence, TDC has been rightly questioned whether the constant gain can guarantee the best performance spanning dynamic situations of the robot. More specifically, its inertial parameters can significantly vary when the joint configuration is changed during the operation, and uncertain external disturbances can also be applied to the end-effector; it is then required that the gain matrix $\overline{\mathbf{M}}$ spontaneously adapts to new situations.

To provide a gain self-tuning algorithm for TDC, the authors in [4] slightly modifies the Nussbaum gain technique and uses it together with TDC for a single-input-single-output (SISO) system. However, this technique is not directly implementable into practical systems since it is vulnerable for noises. Moreover, this technique for TDC [4] introduces a number of control design parameters, and the overall performance is heavily dependent on chosen values of the parameters. Consequently, realization of the modified Nussbaum gain method is not easy due to its complexity and noise sensitivity.

In this paper, we present a self-tuning algorithm for the gain of TDC that is computer implementable, low-complexity, and free of noise sensitivity problems. To this end, we reconstruct the conventional TDC formulation using a sliding variable and the TDE, and a self gain-adaptation law inspired by the Plestan's method [21] is exploited. This combination of the sliding-mode-based TDC and adaptive gain dynamics promotes a new formulation of self-tuning TDC (ST-TDC). Incidentally, the difference between the proposed method and Plestan's method lies in the fact that the proposed controller includes the TDE part to compensate uncertain dynamics and disturbances. Stability analysis of the overall dynamics, including the proposed gain dynamics and the modified TDC, is proven. As a consequence, the gain of the TDC is automatically adjusted to accomplish the desired error dynamics described by sliding mode. When the TDE error increases at the point a velocity reversal occurs due to the nonlinear friction, the adaptive gain is automatically increased to counteract the TDE error. The proposed method prevent a too-high value of the gain; thus, chattering problem is avoided. The efficacy of the proposed control is confirmed by a highly accurate tracking performance through experiments with an articulated robot.

The rest of the paper is organized as follows: Section 2 gives a concise review of TDC and the TDE technique. Section 3 proposes a self-tuning method of TDC using a sliding mode based gain dynamics, and shows overall stability analysis of the proposed method, which includes both the sliding mode based TDC and the sliding mode based gain dynamics. In Section 4, the proposed method is verified by experimental results. Finally, Section 5 concludes the paper.

2 Review of TDC and the TDE technique

The dynamics equation of a n-degrees-of-freedom (DoFs) articulated robot is expressed as follows:

$$\boldsymbol{\tau} = \mathbf{M}(\mathbf{q})\ddot{\mathbf{q}} + \mathbf{B}(\mathbf{q}, \dot{\mathbf{q}})\dot{\mathbf{q}} + \mathbf{g}(\mathbf{q}) + \mathbf{f}(\mathbf{q}, \dot{\mathbf{q}}) + \mathbf{d}, \tag{1}$$

where $\boldsymbol{\tau} \in \mathbb{R}^n$ denotes the vector of joint torque, $\mathbf{M}(\mathbf{q}) \in \mathbb{R}^{n\times n}$ represents the inertia matrix of the robot, $\mathbf{q}$,$\dot{\mathbf{q}}$, and $\ddot{\mathbf{q}} \in \mathbb{R}^n$ are vectors of the joint angular position, velocity and acceleration, respectively, $\mathbf{B}(\mathbf{q}, \dot{\mathbf{q}}) \in \mathbb{R}^{n\times n}$ is the Coriolis/centripetal matrix, $\mathbf{g}(\mathbf{q}) \in \mathbb{R}^n$ is the gravity torque vector, $\mathbf{f}(\mathbf{q}, \dot{\mathbf{q}}) \in \mathbb{R}^n$ is the friction force vector, and $\mathbf{d} \in \mathbb{R}^n$ is the disturbance torque vector.

In TDE technique [8, 9, 29], a positive diagonal gain matrix, $\overline{\mathbf{M}} = \mathrm{diag}[\overline{m}_1, \cdots, \overline{m}_n] \in \mathbb{R}^{n\times n}$, is firstly employed to re-express (1) as follows:

$$\overline{\mathbf{M}}\ddot{\mathbf{q}} + \boldsymbol{\psi}(\mathbf{q}, \dot{\mathbf{q}}, \ddot{\mathbf{q}}) = \boldsymbol{\tau}, \tag{2}$$

where

$$\begin{aligned}\boldsymbol{\psi}(\mathbf{q}, \dot{\mathbf{q}}, \ddot{\mathbf{q}}) = [\mathbf{M}(\mathbf{q}) - \overline{\mathbf{M}}]\ddot{\mathbf{q}} + \mathbf{B}(\mathbf{q}, \dot{\mathbf{q}})\dot{\mathbf{q}} + \mathbf{g}(\mathbf{q}) \\ + \mathbf{f}(\mathbf{q}, \dot{\mathbf{q}}) + \mathbf{d}.\end{aligned} \tag{3}$$

The objective of control is to drive the joint angular position of the robot $\mathbf{q}$ to track the desired trajectory $\mathbf{q}_d$. The reference dynamics is thus set as

$$\ddot{\mathbf{e}} + \mathbf{K}_\nu\dot{\mathbf{e}} + \mathbf{K}_\rho\mathbf{e} = \mathbf{0}, \tag{4}$$

where $\mathbf{e} = \mathbf{q}_d - \mathbf{q}$, while $\mathbf{K}_\nu$ and $\mathbf{K}_\rho$ are derivative and proportional gain matrices, respectively. The control input toque is designed as

$$\boldsymbol{\tau} = \overline{\mathbf{M}}\mathbf{v} + \widehat{\boldsymbol{\psi}}(\mathbf{q}, \dot{\mathbf{q}}, \ddot{\mathbf{q}}), \tag{5}$$

$$\mathbf{v} = \ddot{\mathbf{q}}_d + \mathbf{K}_\nu \dot{\mathbf{e}} + \mathbf{K}_\rho \mathbf{e}, \tag{6}$$

where $\widehat{\boldsymbol{\psi}}(\mathbf{q}, \dot{\mathbf{q}}, \ddot{\mathbf{q}})$ represents the estimation of $\boldsymbol{\psi}(\mathbf{q}, \dot{\mathbf{q}}, \ddot{\mathbf{q}})$.

Here, the TDE technique is introduced to estimate the nonlinear control term $\widehat{\boldsymbol{\psi}}(\mathbf{q}, \dot{\mathbf{q}}, \ddot{\mathbf{q}})$ as follows:

$$\widehat{\boldsymbol{\psi}}(\mathbf{q}, \dot{\mathbf{q}}, \ddot{\mathbf{q}}) = \boldsymbol{\psi}(\mathbf{q}, \dot{\mathbf{q}}, \ddot{\mathbf{q}})_{(t-L)}, \tag{7}$$

where $\diamond_{(t-L)}$ denotes the time-delayed value of $\diamond_{(t)}$, and L in the subscription denotes the time delay which is sufficiently small for the estimation. Hereinafter, $(\mathbf{q}, \dot{\mathbf{q}}, \ddot{\mathbf{q}})$ of the function is omitted for brevity of expression. Then, one can obtain the estimation of $\widehat{\boldsymbol{\psi}}$ using (2) as follows:

$$\boldsymbol{\psi}_{(t-L)} = \boldsymbol{\tau}_{(t-L)} - \overline{\mathbf{M}}\ddot{\mathbf{q}}_{(t-L)}, \tag{8}$$

where the acceleration signal is computed by the numerical differentiation as $\ddot{\mathbf{q}}_{(t-L)} = \{\mathbf{q}_{(t)} - 2\mathbf{q}_{(t-L)} + \mathbf{q}_{(t-2L)}\}/L^2$, as a single angle measurement, i.e., encoder, is considered in practice. Thus, with the combination of (5)-(8), the TDC law for the articulated robot is expressed as follows [9]:

$$\boldsymbol{\tau} = \overline{\mathbf{M}}(\ddot{\mathbf{q}}_d + \mathbf{K}_\nu \dot{\mathbf{e}} + \mathbf{K}_\rho \mathbf{e}) + [\boldsymbol{\tau}_{(t-L)} - \overline{\mathbf{M}}\ddot{\mathbf{q}}_{(t-L)}]. \tag{9}$$

Note that the gain $\overline{\mathbf{M}}$ of TDC is to be well-tuned since it is dominant for the control performance and stability, while it is also physically interconnected with the system's inertia matrix. Therefore, the constant gain cannot render the best performance when the robot system undergoes variations of inertial properties such as payload and configuration changes, which are often encountered in practical operation scenarios.

3 Self-tuning Control Using the Plestan's Method

3.1 Modification of TDC Employing Sliding Mode Concept

To devise an self-tuning algorithm for the gain of TDC, in this paper, the Hsia's original formulation of the TDC [9] is slightly modified to apply a sliding-mode control concept.

A sliding variable for the n-joint articulated robot is defined as

$$\mathbf{s} = \dot{\mathbf{e}} + \boldsymbol{\lambda}\mathbf{e} \quad \in \mathbb{R}^n, \tag{10}$$

where $\boldsymbol{\lambda} \triangleq \mathrm{diag}[\lambda_1, \cdots, \lambda_n] \in \mathbb{R}^{n\times n}$ is a design matrix governing the sliding surface slope. Then, with $\dot{\mathbf{s}} + \boldsymbol{\lambda}\mathbf{s} = \mathbf{0}$, one can obtain

$$\ddot{\mathbf{e}} + 2\boldsymbol{\lambda}\dot{\mathbf{e}} + \boldsymbol{\lambda}^2\mathbf{e} = \mathbf{0}. \tag{11}$$

The TDC law shown in (9) becomes

$$\boldsymbol{\tau} = \overline{\mathbf{M}}(\ddot{\mathbf{q}}_d + 2\boldsymbol{\lambda}\dot{\mathbf{e}} + \boldsymbol{\lambda}^2\mathbf{e}) + [\boldsymbol{\tau}_{(t-L)} - \overline{\mathbf{M}}\ddot{\mathbf{q}}_{(t-L)}], \tag{12}$$

with $\mathbf{K}_\nu = 2\boldsymbol{\lambda}$ and $\mathbf{K}_\rho = \boldsymbol{\lambda}^2$. Note that the sliding dynamics (11), governed by $\boldsymbol{\lambda}$, forces the closed-loop error quickly converged to zero without oscillation, i.e., critically-damped response [3, 9, 11, 17]. Compared with the conventional formulation (9), the sliding mode based formulation (12) explicitly uses $\mathbf{s}$, which can be regarded as the performance measure of the tracking performance.

Applying the control input (12) and (8) to the robot dynamics (2) yields the closed-loop system dynamics, given by

$$\overline{\mathbf{M}}(\ddot{\mathbf{e}} + 2\boldsymbol{\lambda}\dot{\boldsymbol{e}} + \boldsymbol{\lambda}^2\mathbf{e}) = \boldsymbol{\psi} - \boldsymbol{\psi}_{(t-L)}. \tag{13}$$

Using (10) and (11), the closed-loop error dynamics (13) is re-expressed as follows:

$$\overline{\mathbf{M}}(\dot{\mathbf{s}} + \boldsymbol{\lambda}\boldsymbol{s}) = \boldsymbol{\psi} - \boldsymbol{\psi}_{(t-L)}. \tag{14}$$

If $\boldsymbol{\psi}$ is assumed to be identical to $\boldsymbol{\psi}_{(t-L)}$, the closed-loop equation (11) is equal to the desired error dynamics. Whereas, nonlinear effects generally induce $\boldsymbol{\psi} \neq \boldsymbol{\psi}_{(t-L)}$. The TDE error $\boldsymbol{\varepsilon}$ is thus defined as

$$\boldsymbol{\varepsilon} \triangleq \boldsymbol{\psi} - \boldsymbol{\psi}_{(t-L)}. \tag{15}$$

The sufficient stability condition for TDC is well-established by Yocef-Toumi [30] and Hsia [7], independently:

$$\left\|\mathbf{I} - \mathbf{M}^{-1}\overline{\mathbf{M}}\right\| < 1. \tag{16}$$

When the closed loop system is stable under the stability criterion (16), the TDE error is bounded since $\boldsymbol{\psi}$ consists of continuous system dynamics terms and bounded discontinuous ones [7, 14].

From (14), (15), the closed loop system dynamics with the modified TDC (12) becomes

$$\dot{\mathbf{s}} + \lambda\mathbf{s} = \overline{\mathbf{M}}^{-1}\boldsymbol{\varepsilon}. \tag{17}$$

The TDE error (15) is close to zero in most of the time, but it exhibits a pulse-type signal at velocity reversal because of the Coulomb friction [14]. If $\overline{\mathbf{M}}$ is too small, the size of the tracking error increases because the magnitude of the sliding variable $\mathbf{s}$ becomes large. However, too large $\overline{\mathbf{M}}$ is not preferred either, because noisy performance or chattering can be invoked by the

excessively large value of $\overline{\mathbf{M}}$ [11,14]. Therefore, tuning of $\overline{\mathbf{M}}$ has been regarded as a *compromise problem* between the TDE error and the noise effect. Generally, $\overline{\mathbf{M}}$ of the TDC is constant and tuned heuristically in many conventional researches. An self-tuning algorithm is requested to obtain robust tracking performances within guaranteed accuracy, yet without control input chattering.

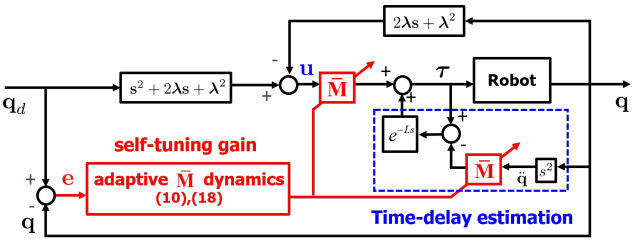

Fig. 1 The block diagram of the proposed self-tuning TDC algorithm.

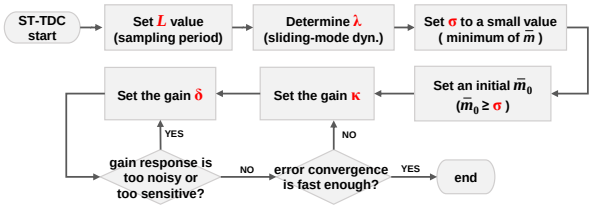

Fig. 2 The flow chart of the implementation process for ST-TDC algorithm.

3.2 Self-tuning Algorithm for TDC

Different from conventional researches [7,9,29], in this paper, $\overline{\mathbf{M}}$ is not a constant matrix. With the proposed modified formulation of the TDC (12), we propose the self-tuning method for TDC using the adaptive law, motivated from Plestan's method [21], as follows:

$$\dot{\overline{m}}_i = \begin{cases} \kappa_i \, |\mathrm{s}_i| \, \mathrm{sgn}(\, |\mathrm{s}_i| - \delta_i) & , \text{if} \quad \overline{m}_i > \sigma \\ \sigma & , \text{if} \quad \overline{m}_i \leq \sigma \end{cases} \tag{18}$$

where $\overline{m}_i$ denotes the i-th element of the diagonal gain $\overline{\mathbf{M}}$, and $\dot{\overline{m}}_i$ denotes its time derivative, while $\kappa_i{>}0$ is the i-th diagonal element of an adaptation gain matrix $\boldsymbol{\kappa} \triangleq \mathrm{diag}[\kappa_1, \cdots, \kappa_n] \in \mathbb{R}^{n\times n}$, $\{\mathbf{sgn}(\mathbf{s})\}_i = \mathrm{sgn}(s_i)$, $\delta_i > 0$, and $\sigma > 0$ is a small constant number. The block diagram of the proposed algorithm is illustrated in Fig. 1 and its implementation process can be summarised as the flow chart in Fig. 2.

The Plestan's method was originally proposed for SISO system [21], and it cannot be directly applied to control of the articulated robot with multiple joints, which is a multi-input-multi-output (MIMO) system, due to the complexity of the robot dynamics. This paper develops an adaptive sliding-mode-based TDC for the robot, i.e., the MIMO system. Another difference between the proposed method and Plestan's method lies in the fact that the proposed algorithm is incorporated with the TDE technique. Thanks to the TDE element, the proposed scheme (12), (18) does not require to calculate robot dynamics equations such as Coriolis/centripetal forces, frictions, and the gravity terms.

As shown in Fig. 1, the proposed method consist of the TDE block, the sliding mode block, and the gain dynamics block. Therefore, it is required to prove the stability of the overall closed loop system controlled by the modified TDC (12) and the gain dynamics (18) and (10). The stability analysis also offers an intuition to set gains of the proposed ST-TDC algorithm shown in Fig. 2.

3.3 Stability Analysis

First, suppose $|s_i| > \delta_i$. $\overline{\mathbf{M}}$ is monotonically increasing according to (18). Considered Lyapunov function as

$$V = 0.5\mathbf{s}^T\mathbf{s} + 0.5\sum_{i=1}^{n}(\overline{m}_i - \overline{m}_i^\star)^2, \tag{19}$$

where $\overline{m}_i^\star$ is the i-th element of a positive diagonal matrix $\overline{\mathbf{M}}^\star$ presumed to be existed in the range of $\overline{\mathbf{M}}$. The time derivative of V is given as

$$\begin{aligned} \dot{V} &= \mathbf{s}^T\dot{\mathbf{s}} + \sum_{i=1}^{n}(\overline{m}_i - \overline{m}_i^\star)\dot{\overline{m}}_i \\ &= \mathbf{s}^T(-\boldsymbol{\lambda}\boldsymbol{s} + \overline{\mathbf{M}}^{-1}\boldsymbol{\varepsilon}) \\ &\quad + \sum_{i=1}^{n}[(\overline{m}_i - \overline{m}_i^\star)\kappa_i|s_i|\mathrm{sgn}(|s_i| - \delta_i)], \end{aligned} \tag{20}$$

and this yields

$$\begin{aligned} \dot{V} &= \sum_{i=1}^{n}[(-\lambda_i s_i^2 + s_i\overline{m}_i^{-1}\varepsilon_i) + (\overline{m}_i - \overline{m}_i^\star)\kappa_i|s_i|] \\ &\leq \sum_{i=1}^{n}\{-\lambda_i|s_i|^2 + |s_i|[\overline{m}_i^{-1}|\varepsilon_i| + (\overline{m}_i - \overline{m}_i^\star)\kappa_i]\}. \end{aligned} \tag{21}$$

The time derivative of V is negative, if $\overline{m}_i^{-1}|\varepsilon_i| + (\overline{m}_i - \overline{m}_i^\star)\kappa_i < 0$. Referring the inequality condition $ax^{-1} + bx \geq 2\sqrt{ab}$ holds if $x > 0$ and $a, b > 0$, one can find the lower bound of the gain $\overline{\mathbf{M}}$ as

$$\overline{m}_i^\star \geq 2\sqrt{\kappa_i^{-1}|\varepsilon_i|} \triangleq \overline{m}_i{}^{\ominus}. \tag{22}$$

This infers that $|s_i|$ can be increased, if $\overline{m}_{i(t=0)} < \overline{m}_i{}^{\ominus}$. However, note that $\overline{m}_i$ is increasing so that it has to

become larger than $\overline{m}_i^{\ominus}$ in a certain time; thus, there exists a finite time such that the gain $\overline{\mathbf{M}}$ is sufficiently large to make the sliding variable $|s_i|$ decreasing according to the closed-loop dynamics (17).

In order to obtain the upper bound of the gain $\overline{\mathbf{M}}$, consider Lyapunov function as $V = 0.5\mathbf{s}^T\mathbf{s}$. $\dot{V}$ is given as $\dot{V} = \mathbf{s}^T\dot{\mathbf{s}} = \mathbf{s}^T(\overline{\mathbf{M}}^{-1}\boldsymbol{\varepsilon} - \boldsymbol{\lambda}\mathbf{s})$. One then can obtain $\dot{V} < 0$ under the condition $|s_i| > |\varepsilon_i||\lambda_i\overline{m}_i|^{-1}$. Since $|\varepsilon_i|$ is bounded as addressed in (15), the ultimate bound of $|s_i|$ is $|\varepsilon_i||\lambda_i\overline{m}_i^{\star}|^{-1}$. That is,

$$\overline{m}_i^{\star} \leq |\varepsilon_i||\lambda_i\delta_i|^{-1} \triangleq \overline{m}_i^{\oplus}. \tag{23}$$

Apparently, it follows that $|s_i| < \delta_i$ in a finite time after $\overline{m}_i$ reaches to a maximum value. The inequality $\overline{m}_i^{\oplus} > \overline{m}^{\ominus}{}_i$ has to be satisfied; thus, when selecting gains, the condition $\kappa_i > 4|\lambda_i\delta_i|^2|\varepsilon_i|^{-1}$ should be satisfied.

Second, suppose $|s_i| \leq \delta_i$. Equation (18) yields that $\overline{\mathbf{M}}$ is monotonically decreasing. The Lyapunov function is taken as follows:

$$V = 0.5\mathbf{s}^T\mathbf{s} + \sum_{i=1}^{n}\left|\overline{m}_i - \overline{m}_i^{\oplus}\right|, \tag{24}$$

and its time derivative is expressed as

$$\begin{aligned}\dot{V} &= \mathbf{s}^T\dot{\mathbf{s}} + \sum_{i=1}^{n}\dot{\overline{m}}_i\mathrm{sgn}(\overline{m}_i - \overline{m}_i^{\oplus}) \\ &= \sum_{i=1}^{n}(-\lambda_i s_i^2 + s_i\overline{m}_i^{-1}\varepsilon_i) + \sum_{i=1}^{n}(\kappa_i|s_i|) \\ &\leq \sum_{i=1}^{n}\{-\lambda_i|s_i|[|s_i| - \lambda_i^{-1}(\overline{m}_i^{-1}|\varepsilon_i| + \kappa_i)]\}.\end{aligned} \tag{25}$$

If $|s_i| > \lambda_i^{-1}(\overline{m}_i^{-1}|\varepsilon_i| + \kappa_i)$, $\dot{V}$ is negative; this means that the sliding variable can be bounded in the region $|s_i| \leq \lambda_i^{-1}\rho_i$, where $\rho_i \triangleq \overline{m}_i^{-1}|\varepsilon_i| + \kappa_i$. Note that if the gain $\overline{\mathbf{M}}$ becomes too small to sufficiently compensate the robot dynamics with uncertainties, it leads the bounded region ρ_i becomes enlarged over δ_i and the sliding variable increases. Indeed, once $|s_i| > \delta_i$, the process restarts from the beginning. Therefore, the boundedness of the sliding variable $|s_i| \leq \lambda_i^{-1}\rho_i$ is guaranteed for any $\boldsymbol{\delta}$, which completes the stability analysis of the overall system. The consistent result of the process governed by the adaptive self-tuning gain $\overline{\mathbf{M}}$ can be physically observed in experimental results shown in the following section.

4 Experimental Studies

4.1 Settings

The proposed self-tuning TDC (ST-TDC) with the adaptive sliding-mode-based gain dynamics is realized and compared with the well-tuned conventional TDC (9). The system employed in the experiment is the robot named 'cCub' [22] shown in Fig. 3, where a single leg has six DoFs with the configuration of pitch-roll-yaw-pitch-pitch-roll joints from the hip to the foot, thereby a total of 12-DoFs for the entire robot. In this paper, the robot is mounted at a stationary base for the experiment, and position controllers are applied to three pitch joints, i.e., hip (Joint 1), knee (Joint 2) and ankle joints (Joint 3), while others are kept to be in zero angles; hence, six joints of two legs are simultaneously controlled in experiments, while the only data of the right one is presented due to the similarity of results in both legs.

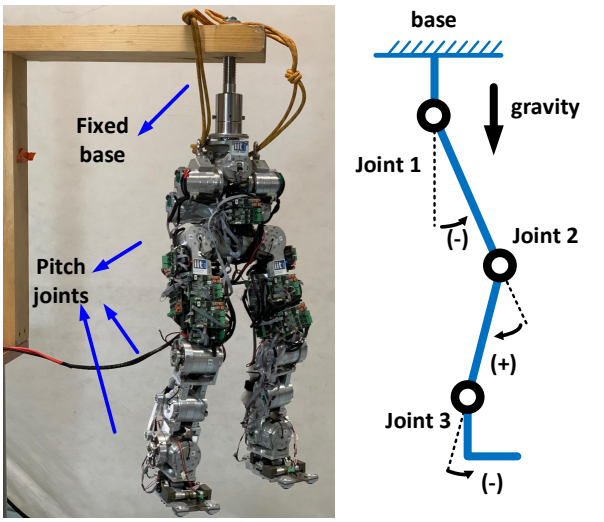

Fig. 3 The experimental setup: the articulated robot cCub is set with a fixed base, where the three pitch joints are controlled while the other joints are immobilized without control (left); the schematic diagram (right) presents the joint numbers, direction of the angles with ± signs, and the zero angle configuration with dashed lines.

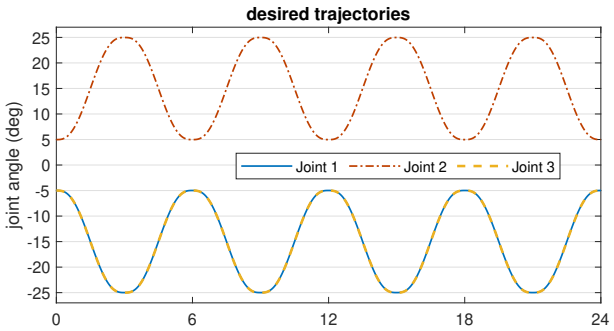

Fig. 4 The desired position trajectories for three joints created by the fifth-order polynomial function.

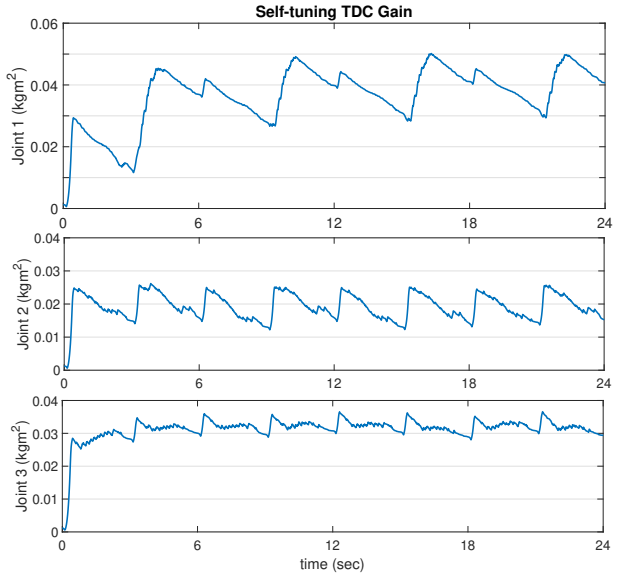

Fig. 5 The responses of the proposed ST-TDC gains $\overline{\mathbf{M}}$.

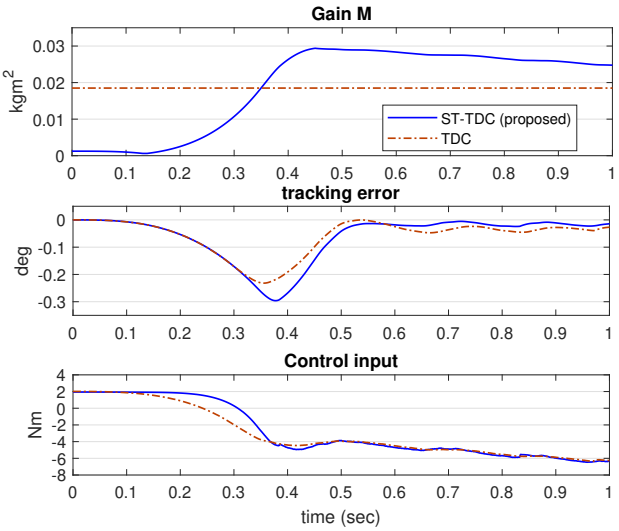

Fig. 6 Transient responses t = 0-0.5s of comparative experiments with conventional TDC (dashed line) and the proposed ST-TDC (solid line): $\overline{\mathbf{M}}$, tracking errors, and control inputs of the joint 1 (those of other joints are omitted since the same trend is observed.)

At each joint, the magnetic encoder with a resolution of 13-bit is mounted before the gear train with a reduction of 100:1; and the individual joint is equipped with an embedded micro-controller generating the control torque. The hard realtime control system is implemented with Simulink Real-Time$^{\text{TM}}$, communicating with micro-controllers in each joint of the robot through EtherCAT connection with a sampling rate of 1 kHz, i.e., $L = 0.001$ is set in the controllers.

All of the joints are commanded by the same fifth-order trajectory as shown in Fig. 4 which is assigned to periodically move 20 degrees in every 3 seconds. The same error dynamics $\ddot{\mathbf{e}} + (2 \cdot 24)\dot{\mathbf{e}} + 24^2\mathbf{e} = \mathbf{0}$ is used for comparison with the conventional TDC, i.e., $\boldsymbol{\lambda} = \text{diag}[24, 24, 24]$. The constant TDC gain $\overline{\mathbf{M}}$ are elaborately tuned to achieve the best tracking by trial and error method and a well-tuned gain is finally found as $\overline{\mathbf{M}} = \text{diag}[0.0185, 0.0154, 0.0154]$ kgm^2. Whereas, parameters for the proposed self-tuning method of $\overline{\mathbf{M}}$, (18), are selected as $\boldsymbol{\kappa} = \text{diag}[0.2, 0.2, 0.2]$, $\sigma = 0.00005$, and $\boldsymbol{\delta} = [0.015, 0.015, 0.015]^T$.

Remark 1 For the initial values of the proposed self-tuning gain, it is recommended to set nominal values of $\mathbf{M}$ within operating ranges if users has prior knowledge of the inertial parameters. Nevertheless, in this experiment, it is *intentionally* set to a very small value to consider practical situations; the small initial value mimics such cases when one assign small values due to the lack of prior knowledge of system parameters, or when $\mathbf{M}$ is suddenly and severely changed, e.g., payload addition/removal.

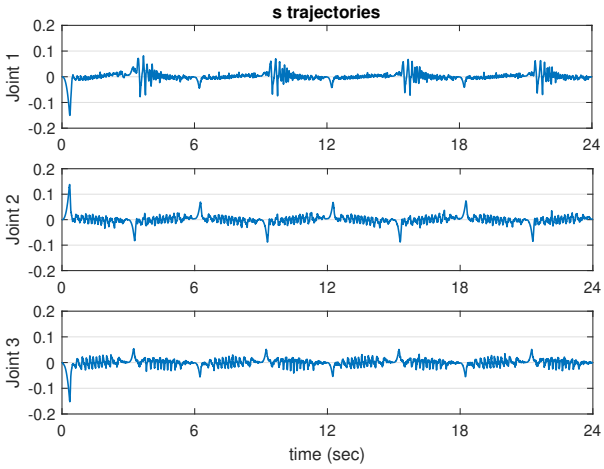

Fig. 7 The trajectories of sliding variables $\mathbf{s}$ of the proposed method.

4.2 Results

Figs. 5-8 present the entire experimental results. The root-mean squared (RMS) values of the tracking errors are encapsulated in Table 1, where the values in parentheses denote those during the initial transient period of the gain adaption (t=0-0.5s). As shown in Fig. 5, the proposed ST-TDC gain is quickly increased from 0 to appropriate values within a short time period, when $|s_i| \geq \delta_i$. Note that in the transient region $t < 0.5$s as seen in Fig. 6 and Table 1, RMS tracking errors of the proposed control are larger than those of the conventional TDC because the initial values of $\overline{\mathbf{M}}$ for the pro-

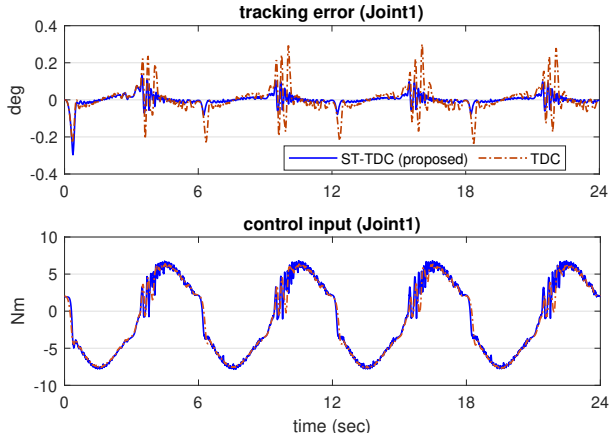

(a)

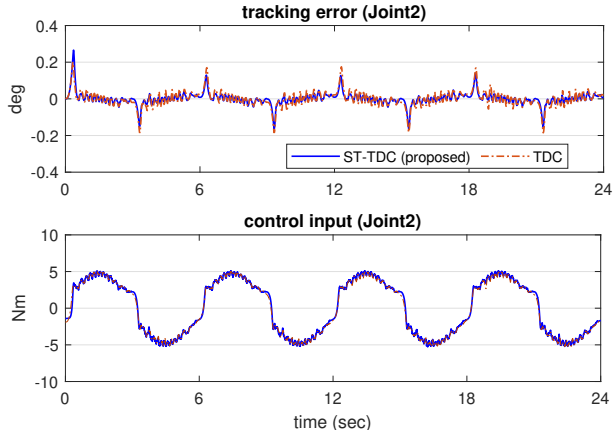

(b)

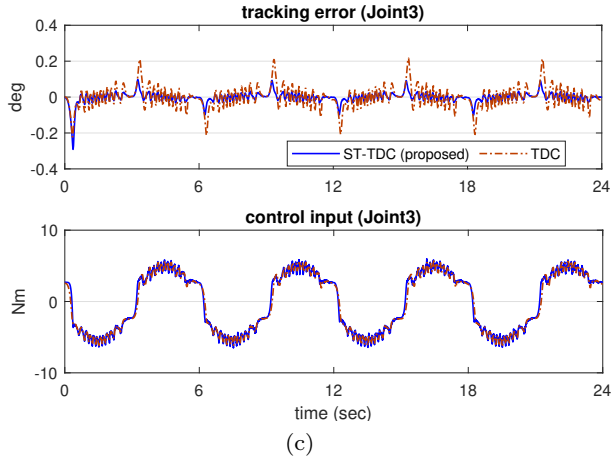

(c)

Fig. 8 Comparative experiment results of tracking errors and control inputs with the conventional TDC (red dash-dotted line) and the proposed ST-TDC (blue solid line).

posed control are set to be very small (e.g., zero in this experiment) and the gains are being updated; one can observe in Fig. 7 that the sliding variable $\mathbf{s}$ is increased as $\overline{\mathbf{M}}$ is too small. Whereas, owing to the adaptation of $\overline{\mathbf{M}}$, the proposed control clearly outperforms the TDC

Table 1 RMS tracking errors [t =0.5-24s (0-0.5s) $\times 10^{-3}$ deg].

Controller	Joint 1	Joint 2	Joint 3
Proposed ST-TDC	**0.414**	**0.522**	**0.379**
	(**2.522**)	(**2.182**)	(**2.426**)
Conventional TDC	1.157	0.715	0.967
	(2.082)	(1.670)	(1.915)

after the transient period $t \geq 0.5$s. One can also observe that $\mathbf{s}$ is well-bounded, when $\overline{\mathbf{M}}$ is being updated. Note that some peaks are observed in the $\mathbf{s}$ trajectories and the tracking errors, which are caused by the friction when the joint velocity crosses zero, since the rapid dynamics of the static and Coulomb frictions creates large tracking errors. The TDE error $\boldsymbol{\varepsilon}$ exhibits a pulse-type disturbance due to discontinuity of Coulomb friction at the point of the velocity reversal occurs. It is worth to notice that the gain $\overline{\mathbf{M}}$ increases at the point of the velocity reversal as depicted in Fig. 5 in order to compensate the aforementioned TDE error from the discontinuous friction torques. Accordingly, the adaptive gain is increased to force the term $\overline{\mathbf{M}}^{-1}\varepsilon$ reduced in the error dynamics $(\dot{\mathbf{s}} + \lambda\mathbf{s}) = \overline{\mathbf{M}}^{-1}\varepsilon$. This leads the automatic-tuned TDC with the the proposed adaptive method achieves smaller steady-state errors compared with the conventional TDC with the constant gain as shown in Figs. 8a, 8b, and 8c.

The oscillation in the $\overline{\mathbf{M}}$ response in the time interval 3s<t<24s is originated from the nature of $\overline{\mathbf{M}}$ dynamics. As seen in (18), when $|s_i| \geq \delta_i$, the $\overline{\mathbf{M}}$ increases promptly; and when $|s_i| < \delta_i$, the $\overline{\mathbf{M}}$ slowly decreases. As a result, the $\overline{\mathbf{M}}$ dynamics ensures the tracking of $\mathbf{s}$ trajectory within some precision, rather than perfect tracking. Too high value of gain is prevented by the $\overline{\mathbf{M}}$ dynamics; thus, chattering is avoided.

It is worth to notice that the proposed controller as well as TDC use acceleration signals for dynamics estimation, e.g., TDE, as an expense of the model-parameter-free nature. Although the acceleration signal obtained from the numerical differentiation is very noisy, one can observe a certain trend that the desired acceleration trajectory is tracked by both controllers as shown in Fig. 9a. To present clearer comparison of the responses, we analyse the velocity error, which equals to the values of the numerical integration of the acceleration error. As seen in Fig. 9b, it is confirmed that the tracking result of the proposed ST-TDC is better, where its RMS value after the transient period (t≥0.5s) is 0.506 deg/s while that from TDC is 0.880 deg/s.

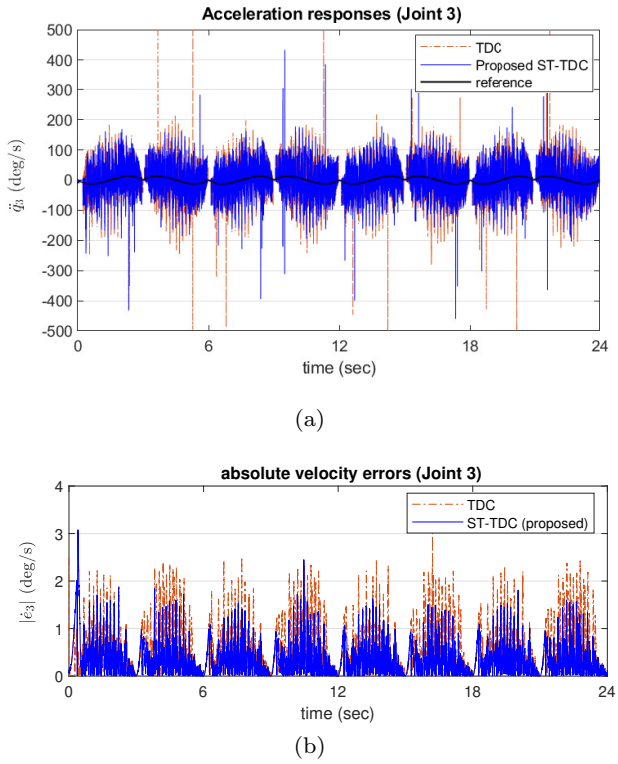

Fig. 9 Experiment results of acceleration tracking and velocity tracking errors at Joint 3, with the conventional TDC and the proposed ST-TDC (those from Joints 1,2 are omitted due to similarity and for brevity).

5 Conclusion

Adaptive techniques are developed to automatically tune the gain of TDC for the multiple DoFs articulated robot. The modified formulation of the TDC law proposed in this paper explicitly relates the $\overline{\mathbf{M}}$ to the tracking error through the sliding mode based reference dynamics. The overall closed-loop system with the TDE and the adaptive self-tuning gain dynamics is stable. The gain is dynamically adjusted to achieve the desired error dynamics. The effectiveness of the proposed self-tuning TDC method is experimentally verified by controlling six joints of the robot. The gain adaptation method for TDC automatically renders appropriate values for each joints in $\overline{\mathbf{M}}$ that achieves accurate tracking performance without control chattering. As the conventional TDC requires laborious manual tuning which is ended up with constant values, one cannot be easily convinced if the resulting constant gains are the best throughout the dynamic operation scenario with the several joints. The proposed method can provide well-tuned time varying gains as a confident and automatic resolution.

References

1. Bae, H.J., Jin, M., Suh, J., Lee, J., Chang, P.H., Ahn, D.S.: Control of robot manipulators using time-delay estimation and fuzzy logic systems. J. Elect. Eng. Technol. **12**(3), 1271–1279 (2017)
2. Baek, J., Kwon, W., Kang, C.: A new widely and stably adaptive sliding-mode control with nonsingular terminal sliding variable for robot manipulators. IEEE Access **8**, 43443–43454 (2020)
3. Chang, P.H., Lee, J.W.: A model reference observer for time-delay control and its application to robot trajectory control. IEEE Transactions on Control Systems Technology **4**(1), 2–10 (1996)
4. Cho, S.J., Jin, M., Kuc, T.Y., Lee, J.S.: Stability guaranteed auto-tuning algorithm of a time-delay controller using a modified Nussbaum function. International Journal of Control **87**(9), 1926–1935 (2014)
5. Cho, S.J., Lee, J., Kim, J., Kuc, T.Y., Chang, P.H., Jin, M.: Adaptive time-delay control with a supervising switching technique for robot manipulators. Trans. Inst. Meas. Control **39**(9), 1374–1382 (2017)
6. Geng, J., Sheng, Y., Liu, X.: Time-varying nonsingular terminal sliding mode control for robot manipulators. Transactions of the Institute of Measurement and Control **36**(5), 604–617 (2014)
7. Hsia, T., Gao, L.: Robot manipulator control using decentralized linear time-invariant time-delayed joint controllers. In: 1990 IEEE International Conference on Robotics and Automation, pp. 2070–2075. IEEE (1990)
8. Hsia, T.C.: A new technique for robust control of servo systems. IEEE Transactions on Industrial Electronics **36**(1), 1–7 (1989)
9. Hsia, T.C., Lasky, T.A., Guo, Z.: Robust independent joint controller design for industrial robot manipulators. IEEE Transactions on Industrial Electronics **38**(1), 21–25 (1991)
10. Jin, M., Chang, P.H.: Simple robust technique using time delay estimation for the control and synchronization of lorenz systems. Chaos, Solitons & Fractals **41**(5), 2672–2680 (2009)
11. Jin, M., Kang, S.H., Chang, P.H.: Robust compliant motion control of robot with nonlinear friction using time-delay estimation. IEEE Transactions on Industrial Electronics **55**(1), 258–269 (2008)
12. Jin, M., Kang, S.H., Chang, P.H., Lee, J.: Robust control of robot manipulators using inclusive and enhanced time delay control. IEEE/ASME Transactions on Mechatronics **22**(5), 2141–2152 (2017)
13. Jin, M., Lee, J., Ahn, K.K.: Continuous nonsingular terminal sliding-mode control of shape memory alloy actuators using time delay estimation. IEEE/ASME Transactions on Mechatronics **20**(2), 899–909 (2015)
14. Jin, M., Lee, J., Chang, P.H., Choi, C.: Practical nonsingular terminal sliding-mode control of robot manipulators for high-accuracy tracking control. IEEE Transactions on Industrial Electronics **56**(9), 1406–1414 (2009)
15. Kim, Y.B.: Improving dynamic performance of proton-exchange membrane fuel cell system using time delay control. Journal of Power Sources **195**(19), 6329 – 6341 (2010)
16. Lee, J., Chang, P.H., Jamisola, R.S.: Relative impedance control for dual-arm robots performing asymmetric bimanual tasks. IEEE Transactions on Industrial Electronics **61**(7), 3786–3796 (2014)

17. Lee, J., Dallali, H., Jin, M., Caldwell, D.G., Tsagarakis, N.G.: Robust and adaptive dynamic controller for fully-actuated robots in operational space under uncertainties. Autonomous Robots **43**(4), 1023–1040 (2019)
18. Lee, J., Deshpande, N., Caldwell, D.G., Mattos, L.S.: Microscale precision control of a computer-assisted transoral laser microsurgery system. IEEE/ASME Transactions on Mechatronics **25**(2), 604–615 (2020)
19. Lee, J., Yoo, C., Park, Y.S., Park, B., Lee, S.J., Gweon, D.G., Chang, P.H.: An experimental study on time delay control of actuation system of tilt rotor unmanned aerial vehicle. Mechatronics **22**(2), 184–194 (2012)
20. Lewis, F.L., Abdallah, C.T., Dawson, D.: Control of Robot Manipulators. New York: Macmillan (1993)
21. Plestan, F., Shtessel, Y., Bregeault, V., Poznyak, A.: New methodologies for adaptive sliding mode control. International Journal of Control **83**, 1907–1919 (2010)
22. Tsagarakis, N.G., Li, Z., Saglia, J., Caldwell, D.G.: The design of the lower body of the compliant humanoid robot cCub. In: proc. IEEE Int. Conf. Robot. Autom., pp. 2035–2040. IEEE (2011)
23. Wang, X., Niu, R., Chen, C., Zhao, J.: H_∞ switched adaptive control for a class of robot manipulators. Transactions of the Institute of Measurement and Control **36**(3), 347–353 (2014)
24. Wang, Y., Meng, S., Ju, F., Chen, B., Wu, H.: A novel model-free robust control of cable-driven manipulators. IEEE Access **7**, 125532–125541 (2019)
25. Wang, Y., Yan, F., Chen, J., Chen, B.: Continuous nonsingular fast terminal sliding mode control of cable-driven manipulators with super-twisting algorithm. IEEE Access **6**, 49626–49636 (2018)
26. Wang, Y., Yan, F., Ju, F., Chen, B., Wu, H.: Optimal nonsingular terminal sliding mode control of cable-driven manipulators using super-twisting algorithm and time-delay estimation. IEEE Access **6**, 61039–61049 (2018)
27. Wang, Y., Zhu, K., Chen, B., Jin, M.: Model-free continuous nonsingular fast terminal sliding mode control for cable-driven manipulators. ISA Transactions **98**, 483 – 495 (2020)
28. Wang, Y.X., Xuan, D.J., Kim, Y.B.: Design and experimental implementation of time delay control for air supply in a polymer electrolyte membrane fuel cell system. International Journal of Hydrogen Energy **38**(30), 13381 – 13392 (2013)
29. Youcef-Toumi, K., Ito, O.: A time delay controller for systems with unknown dynamics. ASME Journal of Dynamic Systems, Measurement, and Control **112**(1), 133–142 (1990)
30. Youcef-Toumi, K., Wu, S.T.: Input/output linearization using time delay control. ASME Journal of Dynamic Systems, Measurement, and Control **114**(1), 10–19 (1992)